Immobilization of Thermoalkalophilic Esterase Onto Magnetic-Cornstarch Nanoparticle

Yasin Öz
Izmir Institute of Technology: Izmir Yuksek Teknoloji Enstitusu
Yusuf Sürmeli
Izmir Institute of Technology: Izmir Yuksek Teknoloji Enstitusu
Gulsah Sanli-Mohamed (gulsahsanli@iyte.edu.tr)
Izmir Institute of Technology

Research Article

Keywords: thermoalkalophilic esterase, Geobacillus sp., immobilization, magnetic nanoparticles

Posted Date: February 24th, 2021

DOI: https://doi.org/10.21203/rs.3.rs-224390/v1

Abstract

The immobilization of the biocatalysts onto magnetic nanoparticles (MNPs) has been extensively applied since the external magnetic field facilitates the enzyme recovery from the reaction mixture. In the present study, glutaraldehyde-modified magnetite-cornstarch nanoparticles (MCNs) were successfully synthesized, elaborately characterized by ZetaSizer and surface-enhanced raman spectroscopy (SERS), and used for the immobilization of a thermoalkalophilic esterase from *Geobacillus* sp. The optimal immobilization conditions were obtained at 65^{o}C, 2:3 molar ratios of Fe^{2+}:Fe^{3+} and 1 g cornstarch resulted in approximately 90 nm magnetic particles in size. Also, immobilization yield and entrapment efficiency of the esterase were found as 74% and 82%, respectively. Scanning Electron Microscopy (SEM) micrographs showed that MCNs were uniform, spherical in shape, and well dispersed and esterase immobilized MCNs displayed similar morphology as free MCNs. The maximum activity of free and immobilized esterase was obtained at 80^{o}C and pH 9. Immobilization onto glutaraldehyde-modified MCNs significantly enhanced the esterase thermostability. Additionally, the immobilized esterase kept its residual activity of 75% after three sequential cycles, suggesting that it has favorable operational stability.

1. Introduction

Biocatalysts (enzymes) have been largely performed in many bioprocess technologies such as biomedical, biotechnological, and pharmaceutical areas because they possess important catalytic properties including specificity, mild reaction efficacy, and great production yield. Nevertheless, some difficulties continue in terms of their utilization. For instance, the challenges in reusability and recovery of the enzymes are present. Additionally, they have weak stability against reaction conditions (e.g. temperature, pH) and weak activity/selectivity to substrates. To reduce these challenges, an immobilization technique can be used as a powerful strategy to promote these features in biological processes. An immobilized enzyme over free enzyme possesses higher thermostability, operational stability, straightforward enzyme recovery, quick reaction ending, and controlled final product synthesis [1–3].

Various physical and chemical immobilization techniques have been reported using diverse support materials [4]. Recently, among these techniques, the immobilization of the biocatalysts onto magnetic nanoparticles (MNPs) has been extensively applied because of their advantageous properties [5–7]. MNPs enable us to quick and straightforward recovery of the enzyme from the reaction mixture through the external magnetic field. Relative to centrifugation or filtration, the magnetic field creates lower mechanical stress on the immobilized enzyme [8–10]. Immobilization on MNPs also involves several advantages such as a larger surface area to bind more enzyme, lower mass transfer resistance, minor diffusion problem, reduced fouling, lesser operation cost, long term storage and reusability [11–15]. So far, micro- or nano-sized MNPs including chitosan/SiO2 [16], chitosan [17], cellulose [18] and silica [19] have been applied for enzyme immobilization. Cornstarch could be a good candidate as a support material to obtain MNPs for the immobilization of an enzyme [20].

Esterase enzymes (EC 3.1.1.1), which belong to a class of hydrolase, have a bifunctional role. They convert the lipids into carboxylic acid and alcohol, degrading the ester linkages and produce carboxylic ester bonds. The esterases are synthesized by a wide range of organisms including animals, plants, and microorganisms [1]. They act as a substantial part of some applications in biotechnology, industry, environment, and pharmaceutics since they have many beneficial properties [21, 22]. Especially extremozyme esterases possessing exclusive characteristics are of special interest in various reactions [23–25]. Due to their high alkaline and temperature stability, thermoalkalophilic esterases can function at greater performance in some commercial operations [26].

In literature, many studies have been reported various practices of enzyme immobilization using MNPs with various functional groups [27]. Among these, lipases have been immobilized using functionalized MNPs with different groups such as APTES, 2,3-epoxypropyltrimethylammoniumchloride, citric acid, ammonium sülfat, MPTMS, and aniline and ammonium persulfate [28–33]. However, a few reports have been found on esterase immobilization by MNPs. Regarding this, a novel solvent-stable esterase from *Pseudozyma* sp. NII 08165 was immobilized on aminosilane-modified MNPs for biodiesel production [34]. Also, an esterase from *Bacillus pumilus* was immobilized on silane functionalized superparamagnetic iron nanoparticles to synthesize ethyl pyruvate [35]. In addition, another esterase from *Zunongwangia* sp. was immobilized onto magnetite ~ cellulose nano-composite [36]. Beside this, a recombinant esterase from *Pseudomonas putida* IFO12996 was covalently bound to MNPs through glutaraldehyde [37] and hexa-arginine-tagged esterase was immobilized on gold-coated magnetic nanoparticles [38]. Another esterase from *Mucor miehei* was immobilized on core-shell magnetic beads through adsorption and covalent binding for the synthesis of esters [39].

Currently, thermoalkalophilic recombinant *Geobacillus* sp. esterase from Balçova geothermal area has been comprehensively characterized [40]. In addition, it has been immobilized on silicate-coated Ca-alginate using the entrapment method [26]. Nevertheless, to the best of our knowledge, a thermophilic esterase has not been immobilized on glutaraldehyde-modified magnetite-cornstarch nanoparticles (MCNs) in the literature so far. Here, glutaraldehyde-modified MCNs were successfully obtained, characterized in detail by ZetaSizer and SERS, and utilized for the immobilization of a thermoalkalophilic esterase from *Geobacillus* sp. Then, the immobilized esterase was biochemically characterized.

2. Materials And Methods

2.1. Materials

Unless otherwise stated, all chemicals were purchased from Sigma.

2.2. Preparation and characterization of magnetite-cornstarch nanoparticles (MCNs)

2.2.1. Preparation of magnetite-cornstarch nanoparticles (MCNs)

Preparation of magnetite-cornstarch nanoparticles (MCNs) was performed via the method by Wang et al. (2013) with some modifications [20]. For this purpose, $FeCl_3$ and $FeCl_2$ with 2:3 molar ratio were dissolved in 90 mL of dH_2O. 1 g of cornstarch was also dissolved in 10 mL of dH_2O. The cornstarch solution was poured into the $FeCl_3/FeCl_2$ solution and heated in a water bath at 65^oC. The mixture was then adjusted to pH 12–13 by 4 M NaOH and incubated in ultrasonic wave for 20 min. It was stirred at 65^oC for 2 h, cooled to room temperature, and neutralized using acetic acid. Then, the formed precipitate was twice washed using 95% ethanol, gathered via magnetic decantation, and freeze-dried by vacuum freeze-drier. It was stored at 4^oC for further analyses. Co-precipitation of ferrous and ferric ions formed magnetite (Fe_3O_4), which gives the magnetic character to the particles [41] (Fig. 1).

2.2.2. Binding of glutaraldehyde on MCNs

10 mL of 5% of glutaraldehyde solution was prepared in 0.01 M Na-P buffer (pH 7) and 1 g MCNs were supplemented into this solution. The mixture was incubated at 30^oC, 300 rpm for 20 min for the cross-linking process. The precipitate was magnetically collected and washed using 0.01 M Na-P buffer (pH 7). It was then dried via vacuum freezing and stored at 4^oC.

2.2.3. Optimal size distribution of MCNs

The optimal size distribution of MCNs was investigated using DLS (Malvern Zetasizer 3000) by changing different parameters such as temperature, molar ratios of $FeCl_3/FeCl_2$, and quantity of cornstarch. For this purpose, the synthesis of MCNs was performed at four different temperature points (including room temperature, 50^oC, 65^oC, and 80^oC), three different molar ratios of $FeCl_3/FeCl_2$ (1:1, 2:1, and 2:3), and three different quantity of cornstarch (0.8 g, 1.0 g, and 1.2 g). 100 µL of the precipitate was mixed with dH_2O and the sample was analyzed.

2.2.4. SERS analysis of glutaraldehyde-modified MCNs

The composition of glutaraldehyde-modified MCNs was investigated by surface-enhanced raman spectroscopy (SERS) analysis using Raman spectroscopy (Horiba) and the analysis was performed for cornstarch, magnetite, MCNs, and glutaraldehyde-modified MCNs.

2.3. Enzyme preparation

In this study, thermoalkalophilic *Geobacillus* sp. esterase (Est2) previously characterized by Tekedar and Şanlı-Mohamed was utilized [40] was utilized. Heterologous expression of esterase in *Escherichia coli* BL21 (λDE3) and its purification by affinity chromatography were performed as shown in Tekedar and Şanlı-Mohamed (2011) procedure [40]. The further purification of recombinant esterase was carried out by size-exclusion chromatography using a Sephadex G-75 column (Sigma). The purified enzyme was

displayed by 15% SDS-PAGE [42]. Enzyme concentration was quantitatively determined by the Bradford method, using bovine serum albumin (BSA) solutions [43].

2.4. Immobilization of recombinant esterase on glutaraldehyde-modified MCNs

1 g glutaraldehyde-modified MCNs were dissolved in 10 mL of 0.01 M sodium phosphate buffer (pH 8.0) and incubated at 30^{o}C for 30 min. 0.5 mg mL^{-1} esterase was gently supplemented into this solution including MCNs and the mixture was incubated at 30^{o}C, 100 rpm for 4 h. MCNs with esterase were obtained using magnetic decantation, washed with 0.01 M Na-P buffer (pH 7.0), and stored at 4^{o}C until further analyses. Entrapment efficiency (EE) and Immobilization yield (IY) of the enzyme was determined using equations below:

$$EE = \frac{\text{total esterase} - \text{free esterase}}{\text{total esterase}} \times 100 \qquad (1)$$

$$IY = \frac{\text{specific activity of immobilized esterase}}{\text{specific activity of free esterase}} \times 100 \qquad (2)$$

2.5. Characterization of the immobilized esterase

2.5.1. Determination of the activity of the free and immobilized esterase

The activity of the free and immobilized esterase was spectrophotometrically detected by *p*-nitrophenyl acetate (*p*NPA) substrate, which was selected among various *p*-nitrophenyl (*p*-NP) esters having different acyl chain lengths (C2-C16) and kept one of the highest activity [40]. For free enzyme, the assay mixture contained 9 µL of 50 mM *p*NPA, 990 µL of 0.1 M Tris-Cl buffer (pH 9.0), and 1 µL of 1 mg mL^{-1} enzyme. For immobilized enzyme activity, the reaction mixture possessed 10 µL of 50 mM *p*NPA, 980 µL of Tris-Cl buffer (pH 8.0), and 10 µL of 1 mg mL^{-1} enzyme. The activity of the free and immobilized esterases was determined at 55^{o}C, pH 7.2 for 5 min by absorbance measurement at 420 nm. One unit of esterase activity was defined as the amount of enzyme releasing 1 nmol of *p*-nitrophenol per minute.

2.5.2. The influence of pH and temperature

The influence of pH and temperature on the free and immobilized recombinant esterase was analyzed at 90 rpm. The pH effect on the free and immobilized enzymes was studied ranging from 4 to pH 12 at

55^{o}C. The temperature effect on the free and immobilized enzyme was investigated in a range of temperatures (25-90^{o}C) using 0.1 M Tris-Cl buffer (pH 8.0). Standard activity assay was applied to determine the relative activity of the free and immobilized enzyme.

2.5.3. Thermal and pH stability

The analysis for thermal stability was carried out, following incubation for 60 min in a range of temperatures (4-80^{o}C) at pH 8. Also, and pH stability analysis was performed in a range of pH (4–11) at 55^{o}C upon incubation of 60 min. Standard activity assay was applied to determine the residual enzyme activity.

2.5.4. The influence of chemicals

The influence of chemicals including various metal ions at 1 mM concentration ($CaCl_2$, $ZnCl_2$, $MgCl_2$, $CuSO_4$) and two surfactants (1% SDS and 1% Triton X-100) was studied upon incubation of 10 immobilized enzyme beads in 2 mL of 0.1 M Tris-HCl (pH 8.0). Standard activity assay conditions were applied to determine the relative activity of the immobilized enzyme.

2.5.5. Operating stability analysis

Operating stability assay was carried out by practices of seven subsequent standard activity assays of the immobilized enzyme. The beads were washed three times by dH_2O between two consecutive analyses.

2.5.6. Scanning electron micrography (SEM) analysis

The surface morphologies and structure of MCNs and esterase immobilized MCNs were examined by SEM (Philips XL-30S FEG, Eindhoven, The Netherlands).

2.6. Data presentation and statistical analysis

All experiments were carried out in triplicate. Statistical errors of the data were determined by GraphPad Prism version 6.00 for Windows (GraphPad Software, La Jolla, CA, USA) (www.graphpad.com).

3. Results And Discussion

Support structure predominantly influences immobilization performance. Thus, particle size analysis of magnetite-cornstarch nanoparticles (MCNs) was performed under different conditions, showing the influence of temperature (room temperature, 50^{o}C, 65^{o}C, and 80^{o}C), molar ratios of ferrous and ferric ions (2:1, 1:1, and 2:3), and cornstarch quantity (0.8 g, 1 g, and 1.2 g) by ZetaSizer. The analysis results showed that the smallest particle distribution was obtained at 65^{o}C (Fig. 2A). The smallest particle sizes were obtained at 2:3 molar ratio of iron ions where the size

was less than 100 nm, and also at 1 g cornstarch as 90 nm (Figs. 2B and 2C). The small size of magnetic nanoparticles resulted in higher surface area in enzyme immobilization [44].

SERS analysis of glutaraldehyde-modified MCNs was carried out using the surface-enhanced raman spectroscopy (SERS) technique, determining the interactions among starch, magnetite, and glutaraldehyde. SERS analysis results showed that the characteristic raman peaks were determined at 478 cm^{-1} and 2917 cm^{-1} for cornstarch (Fig. 3A), and 668 cm^{-1} for magnetite (Fig. 3B). The peaks of MCNs were determined at the specific points of cornstarch and magnetite (Fig. 3C). For glutaraldehyde-modified MCNs, the number of peaks was increased between 0-1000 cm^{-1} of raman shifts, indicating that glutaraldehyde was bound to the MCN (Fig. 3D).

Free esterase was heterologously expressed in *Escherichia coli* BL21 (DE3) and purified before its immobilization. The enzyme purity was displayed by SDS-PAGE (Fig. 4). The immobilization of the thermoalkalophilic recombinant esterase was performed on glutaraldehyde-modified MCNs. The results showed that immobilization yield and entrapment efficiency were found as 74% and 82%, respectively.

The characterization of the immobilized thermoalkalophilic esterase was performed investigating some parameters such as the influence of pH, temperature, various chemicals, thermostability, and operational stability.

The temperature effect for free and immobilized esterase was studied in a broad range of temperature (25 to 90^{o}C). This analysis showed that both free and immobilized esterase in glutaraldehyde-modified MCNs exhibited maximum activity at 65^{o}C (Fig. 5A). Thus, immobilization of the esterase enzyme in glutaraldehyde-modified MCNs did not change the optimal reaction temperature giving the highest catalytic activity. In one previous work, it was found that the same esterase immobilized using entrapment technique in silicate-coated Ca-alginate beads had an optimum working temperature of 70^{o}C, slightly higher than that of in the present study [26]. There have been several studies on various esterases immobilized by magnetic nanoparticles (MNPs) in the literature. Accordingly, a free esterase of *Bacillus pumilus* exhibited maximum activity at 37^{o}C for free enzyme and 45^{o}C for its immobilized form on silane functionalized superparamagnetic nanoparticles (SNPs) [35]. Another free and immobilized *Zunongwangia* sp. esterase using Fe_3O_4 ~ cellulose nano-composite optimally worked at 30^{o}C and 35^{o}C, respectively [36]. Also, a free *Mucor miehei* esterase and its immobilized form on core-shell magnetic beads through adsorption and covalent binding showed an optimum temperature at 40^{o}C and 50^{o}C, respectively [39]. Similar to the present study, one report has shown that *Pseudomonas putida* IFO12996 esterase immobilization by MNPs exhibited a similar optimal working temperature compared to its free form [37]. In line with this, having a similar optimum temperature of the immobilized and free esterase has been also shown in some reports using different support materials [45, 46].

The pH effect for free and immobilized esterase was investigated in the interval of pH 4 and 11. The analysis showed that both free and immobilized esterase in glutaraldehyde-modified MCNs showed the highest activity at pH 9, exhibiting a similar pH effect profile (Fig. 5B). A previous study demonstrated that immobilization of the same esterase in silicate-coated Ca-alginate beads reduced the optimal pH by one unit, exhibiting maximum activity at pH 8 [26]. Most of the esterase immobilization works using

MNPs did not alter the optimum pH points compared to the free esterases as in the present study [35–37]. Only one study on *Mucor miehei* esterase immobilization using core-shell magnetic beads enhanced the optimal working pH as much as one unit, relative to the free esterase [39].

Thermostability of free and immobilized esterase was studied in a temperature range of 40-80^{o}C for one hour of incubation. The results showed that the immobilized esterase possessed a maximum residual activity at 65^{o}C, higher than that in the free form of the enzyme. Also, the residual activity of free esterase dramatically reduced to 60% and 6% at 70^{o}C and 80^{o}C, respectively. Nevertheless, the immobilized form of the esterase highly kept its residual activity, showing 90% at 70^{o}C and 65% at 80^{o}C after 1 h of incubation (Fig. 6). In previous work, the same thermoalkalophilic esterase entrapped by silicate-coated Ca-alginate beads possessed approximately 60% of residual activity at 80^{o}C upon one hour of incubation [26], showing slightly lower thermal stability compared to the present study. This situation could be associated with esterase position in the immobilization support material. The conformational change of esterase might be constricted by the immobilization matrix without temporarily affecting under denaturant conditions such as high temperatures. Similar to the present study results, three reports have shown that esterase immobilization on different MNP supports including core-shell magnetic beads [39], silane functionalized superparamagnetic nanoparticles (SNPs) [35] and Fe_3O_4 ~ cellulose nano-composite [36] improved thermal stability relative to their free esterases. Only one study has reported that the esterase immobilization process on MNPs did not change the enzyme thermostability [37].

The pH stability was investigated in a range of pH (4–12) upon 1 h of incubation for immobilized esterase in the present study. The results showed that the residual activity of the immobilized enzyme was mostly conserved at alkaline pH points (pH 8–12) after 1 h of incubation, whereas it reduced at acidic pH points (pH 4–6) (data not shown).

The influence of various chemicals on free and immobilized esterase was studied under different metal ion conditions (1 mM $CaCl_2$, 1 mM $ZnCl_2$, 1 mM $MgCl_2$, and 1 mM $CuSO_4$), as well as 1% SDS. This analysis demonstrated that $ZnCl_2$, to some extent, enhanced the immobilized esterase activity, while the other metal ions did not change, except $CuSO_4$ reducing its activity by 10% (Fig. 7). In literature, there have been some reports about the effect of metal ions on esterase immobilized by different support materials. Regarding this, the activity of immobilized esterase (Lx-Est_{BAS}ΔSP) was slightly decreased by Zn^{2+} and increased by Mg^{2+} [47]. Also, Cu^{2+} enhanced and Ca^{2+} sharply reduced another immobilized hNF-*Nm*SGNH1 esterase on hybrid nanoflowers [48]. The present study demonstrated that SDS inactivated the immobilized esterase activity (Fig. 7). In literature, there have been several reports acquiring similar findings to the present study [36, 47–49].

The operational stability of an immobilized biocatalyst is a significant factor for the enzyme utilization in large-scale processes since it declines the operation price. For this reason, the operational stability of the immobilized esterase was analyzed up to seven biocatalyst reaction cycles in 0.1 M Tris-HCl buffer (pH 8.0) at 90 rpm and 55^{o}C for 5 min using *p*NPA substrate. The specific activity was determined after each

cycle during the biocatalyst reaction. The analysis demonstrated that the immobilized esterase kept its residual activity of 75% after three sequential cycles, suggesting that it possesses favorable operational stability (Fig. 8). In one previous study, the same esterase in silicate-coated Ca-alginate beads kept above 72% of the esterase activity following three subsequent cycles [26]. Similar findings have been reported about immobilized esterases on various support materials including MNPs. They have possessed a residual activity of above 70% next three sequential cycles [35, 47–51].

The surface morphology of MCNs and also esterase immobilized onto MCNs was monitored by scanning electron microscopy (SEM) at magnitudes of 2500x and 40x (Fig. 9). Scanning Electron Microscopy (SEM) micrographs showed that MCNs were spherical shape, uniform, and well dispersed. Esterase immobilized MCNs were displayed similar morphology as free MCNs having compact structures.

4. Conclusions

The enzyme immobilization may offer some assistance for industrial processes relative to free enzymes. Among support materials used in enzyme immobilization, magnetic nanoparticles (MNPs) possess the main advantage such as facilitating the enzyme recovery from the reaction mixture using external magnetic field. In the present study, we immobilized a thermoalkalophilic esterase from *Geobacillus* sp. since it is of special interest in different biotechnological processes. Considering this study, glutaraldehyde-modified magnetite-cornstarch nanoparticles (MCNs) were synthesized, the optimal size distribution was determined by Zetasizer, and the components of the MCNs were determined by SERS analysis. The thermoalkalophilic esterase was immobilized onto magnetic nanoparticles as glutaraldehyde-modified MCNs for the first time. The results revealed glutaraldehyde-modified MCNs resulted in 74% of immobilization yield and at least 82% of immobilization efficiency. The immobilization of thermoalkalophilic esterase onto glutaraldehyde-modified MCNs markedly improved the thermal stability. Beside this, it permitted repetitive practices of the esterase with favorable operational stability in a continuous process.

Declarations

Acknowledgments

The authors would like to thank Biotechnology & Bioengineering Research Center at İzmir Institute of Technology for the facilities and technical support.

Ethical Approval

Not applicable.

Consent to Participate

All authors are consent to participate in the manuscript.

Consent to Publish

All authors are consent to publish the manuscript.

Authors Contributions

Yasin Öz: research, methodology, data collection, and writing.

Yusuf Sürmeli: writing—review and editing.

Gülşah Şanlı-Mohamed: research conceptualization, investigation and methodology, supervision, writing—review, and editing.

Funding

Not applicable.

Competing Interests

The authors declare that they have no competing interests.

Availability of data and materials

Not applicable

References

1. Bornscheuer UT. Microbial carboxyl esterases: Classification, properties and application in biocatalysis. Vol. 26, FEMS Microbiology Reviews. No longer published by Elsevier; 2002. p. 73–81.
2. Mozhaev, V. V., Khmelnitsky, Y. L., Sergeeva, M. V., Belova, A. B., Klyachko, N. L., Levashov, A. V. & Martinek, K. (1989). *European Journal of Biochemistry*, *184*, 597–602.
3. Tischer, W. & Kasche, V. (1999). *Trends in Biotechnology*, *17*, 326–335.
4. Ozyilmaz, G. & Yagiz, E. (2012). *Food Chemistry*, *135*(4), 2326–2332.
5. Mahmood, I., Ahmad, I., Chen, G. & Huizhou, L. (2013). *Biochemical Engineering Journal*, *73*, 72–79.
6. Wang, J., Meng, G., Tao, K., Feng, M., Zhao, X., Li, Z., Xu, H., Xia, D. & Lu J. R. (2012). *PLoS ONE*. *7*(8), e43478.
7. Yu, C.-Y., Huang, L.-Y., Kuan, I.-C. & Lee, S.-L. (2013). *International Journal of Molecular Science*, *14*, 24074–24086.
8. Turková, J. (1993). *Journal of Chromatography Library*, *55*, 171–214.
9. Pich, A., Bhattacharya, S., Adler, H. J. P., Wage, T., Taubenberger, A., Li, Z., van Pee, K.-H., Böhmer, U. & Bley, T. (2006). *Macromolecular Bioscience*, *6*(4), 301–310.
10. Ding, Y., Hu, Y., Zhang, L., Chen, Y. & Jiang, X. (2006). *Biomacromolecules*, *7*(6):1766–1772.

11. Perdani, M. S., Juliansyah, M. D., Putri, D. N., Utami, T. S., Hudaya, C., Yohda, M. & Hermansyah, H. (2020). *International Journal of Technology*, *11*(4), 754–763.
12. Dyal, A., Loos, K., Noto, M., Chang, S. W., Spagnoli, C., Shafi, K. V. P. M., Ulman, A., Cowman, M., Gross, R. A. (2003). *Journal of the American Chemical Society*, *125*, 1684–1685.
13. Xie, W. & Ma, N. (2009). *Energy Fuels*, *23*(3), 1347–1353.
14. Liao, M.-H. & Chen, D.-H. (2001). *Biotechnology Letters*, *23*, 1723–1727.
15. Konwarh, R., Karak, N., Rai, S. K. & Mukherjee, A. K. (2009). *Nanotechnology*, *20*(22), 225107.
16. Sahoo, P. C., Jang, Y. N. & Lee, S. W. (2012). *Journal of Molecular Catalysis B: Enzymatic*, *82*, 37–45.
17. Lee, H. U., Song, Y. S., Suh, Y. J., Park, C. & Kim, S. W. (2012). *Journal of Molecular Catalysis B: Enzymatic*, *81*, 31–36.
18. Prikryl, P., Lenfeld, J., Horak, D., Ticha, M. & Kucerova, Z. (2012). *Applied Biochemisty and Biotechnology*, *168*(2), 295-305
19. Zhou, H., Li, W., Shou, Q., Gao, H., Xu, P., Deng, F. & Liu, H. (2012). *Chinese Journal of Chemical Engineering*, *20*(1), 146–151.
20. Wang, B., Cheng, F., Lu, Y., Ge, W., Zhang, M. & Yue, B. (2013). *Journal of Molecular Catalysis B: Enzymatic*, *97*, 137–143.
21. Panda, T. & Gowrishankar, B. S. (2005). *Applied Microbiology and Biotechnology*, *67*, 160–169.
22. Khanna, S., Sekhon, K. K. & Prakash, N. T. (2009). *Biotechnology*, *8*, 235–241.
23. Kim, S. B., Lee, W. & Ryu, Y. W. (2008). *Journal of Microbiology*, *46*, 100–107.
24. Ewis, H. E., Abdelal, A. T. & Lu, C. D. (2004). *Gene*, *329*, 187–195.
25. Kademi, A., Aït-Abdelkader, N., Fakhreddine, L. & Baratti, J. C. (1999). *Enzyme and Microbial Technology*, *24*, 332–338.
26. Gülay, S. & Şanli-Mohamed, G. (2012). *International Journal of Biological Macromolecules*, *50*, 545–551.
27. Bilal, M., Zhao, Y., Rasheed, T. & Iqbal, H. M. N. (2018). *International Journal of Biological Macromolecules*, *120*, 2530–2544.
28. Ali, Z., Tian, L., Zhang, B., Ali, N., Khan, M. & Zhang, Q. (2017). *Enzyme and Microbial Technology*, 103, 42–52.
29. Li, C., Jiang, S., Zhao, X. & Liang, H. (2017). *Molecules*, *22*(1), 179.
30. Li, K., Fan, Y., He, Y., Zeng, L., Han, X. & Yan, Y. (2017). *Scientific Reports*, *7*(1), 1–17.
31. Thangaraj, B., Jia, Z., Dai, L., Liu, D. & Du, W. (2019). *Arabian Journal of Chemistry*, *12*(8), 4694–4706.
32. Cui, J., Cui, L., Jia, S., Su, Z. & Zhang, S. (2016). *Journal of Agricultural and Food Chemistry*, *64*(38), 7179–7187.
33. Mahto, T. K., Chowdhuri, A. R., Sahoo, B. & Sahu, S. K. (2016). *Polymer Composites*, *37*(4), 1152–1160.

34. Alex, D., Mathew, A. & Sukumaran, R. K. (2014). *Bioresource Technology*, *167*, 547–550.
35. Sharma, A., Sharma, T., Meena, K. R., Kumar, A. & Kanwar, S. S. (2018). *Process Biochemistry*, *71*, 109–117.
36. Rahman, M. A., Culsum, U., Kumar, A., Gao, H. & Hu, N. (2016). I*nternational Journal of Biological Macromolecules*, *87*, 488–497.
37. Shaw, S. Y., Chen, Y. J., Ou, J. J. & Ho, L. (2006). *Enzyme and Microbial Technology*, *39*, 1089–1095.
38. Jeong, J., Ha, T. H. & Chung, B. H. (2006). *Analytica Chimica Acta*, *569*(1–2), 203–209.
39. Bayramoglu, G. & Yakup Arica, M. (2014). *Fibers and Polymers*, *15*(10), 2051–2060.
40. Tekedar, H. C. & Şanlı-Mohamed, G. (2011). *Extremophiles*, *15*, 203–211.
41. Kyung Kim, D., Mikhaylova, M., Zhang, Y. & Muhammed, M. (2003). *Chemistry of Materials*, *15*(8), 1617–1627.
42. Laemmli, U. K. (1970). *Nature*, *227*(5259):680–685.
43. Bradford, M. M. (1976). *Analytical Biochemistry*, *72*(1–2), 248–254.
44. Liu, J. F., Liu, H., Tan, B., Chen, Y. H. & Yang, R. J. (2012). *Journal of Molecular Catalysis B: Enzymatic*, *82*, 64–70.
45. Ren, G. & Yu, H. (2011). *Biochemical Engineering Journal*, *53*(3), 286–291.
46. Lee, H., Jeong, H. K., Han, J., Chung, H. S., Jang, S. H. & Lee, C. W. (2013). *Bioresource Technology*, *148*, 620–623.
47. Dong, F., Tang, X., Yang, X., Lin, L., He, D., Wei, W. &Wei, D. (2019). *Catalysts*, *9*(7), 620.
48. Yoo, W., Le, L. T. H. L., Lee, J. H., Kim, K. K. & Kim, T. D. (2019). *Biochimica et Biophysica Acta - Molecular and Cell Biology of Lipids*, *1864*(10), 1438–1448.
49. Kwon, S., Yoo, W., Kim, Y. O., Kim, K. K. & Kim, T. D. (2019). *Biomolecules*, *9*(12), 786.
50. Doraiswamy, N., Sarathi, M. & Pennathur, G. (2019). *Preparative Biochemistry & Biotechnology*, *49*(3), 270–278.
51. Le, L. T. H. L., Yoo, W., Jeon, S., Kim, K. K. & Kim, T. D. (2019). *International Journal of Molecular Sciences*, *21*(1), 91.

Figures

Figure 1

Magnetic aggregation of MCNs by magnets

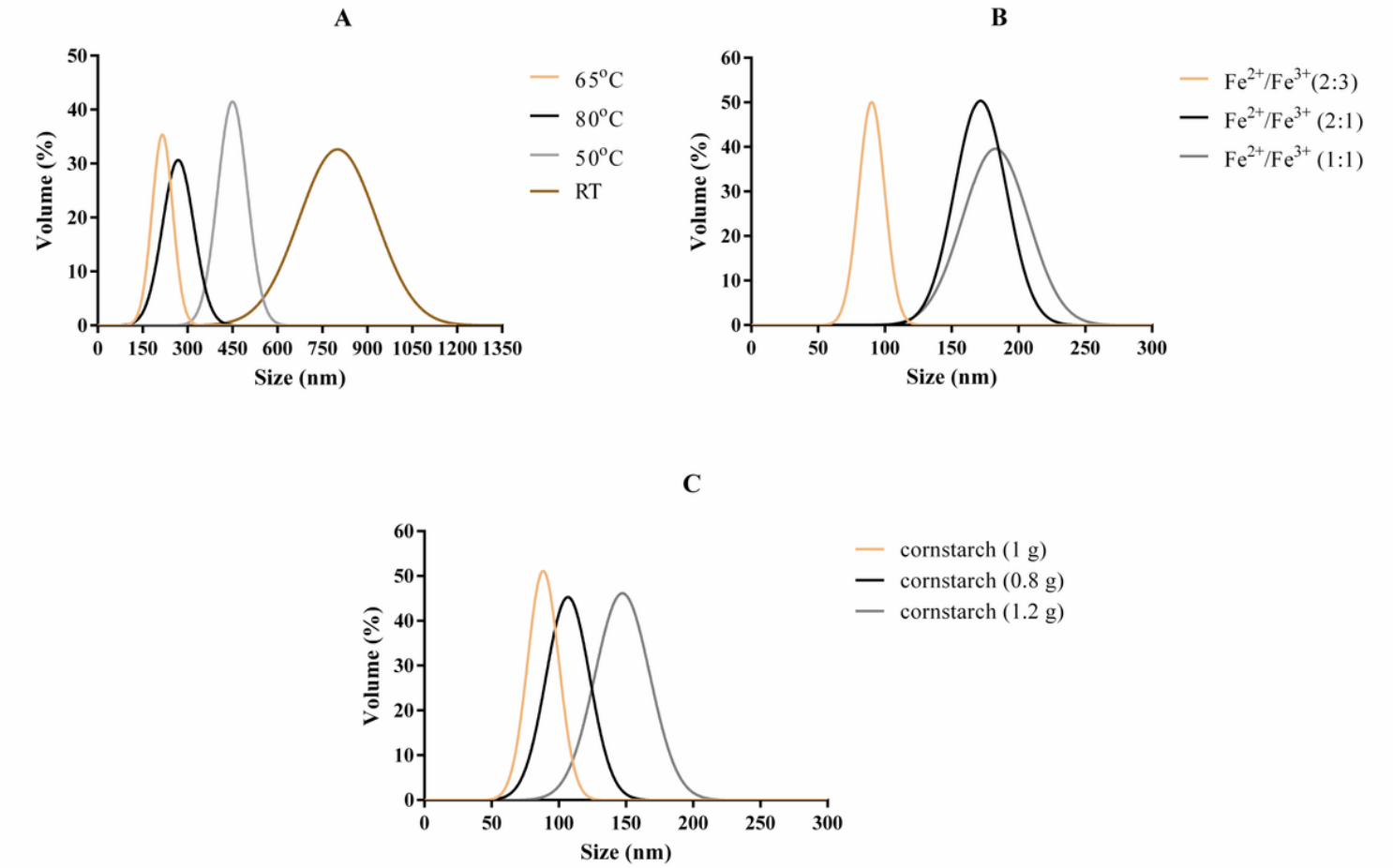

Figure 2

The effect of temperature (A), the molar ratio of magnetite components Fe2+/Fe3+ (B), and the quantity of cornstarch (C) on magnetite-cornstarch particle size distribution. Room temperature was abbreviated as RT.

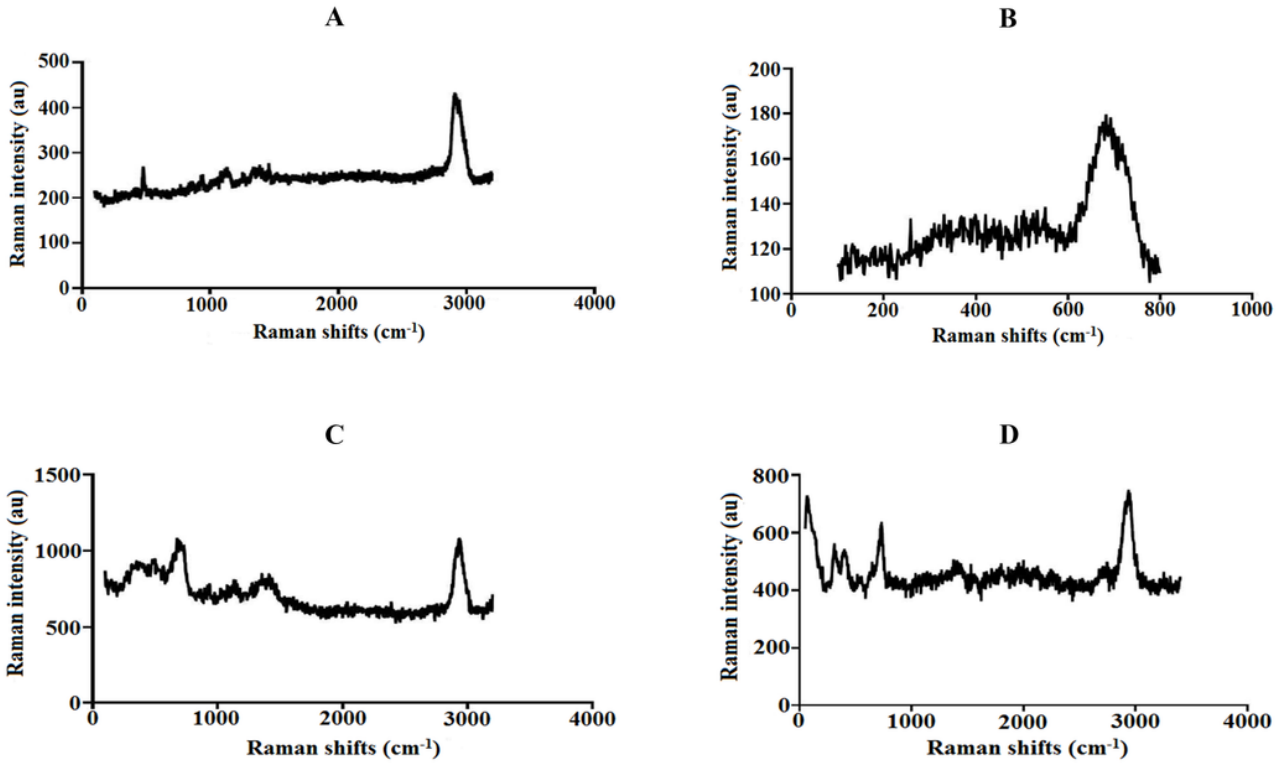

Figure 3

SERS analysis of glutaraldehyde-modified MCNs and their components including cornstarch (A), magnetite (B), cornstarch-magnetite (C), and cornstarch-magnetite-glutaraldehyde (D).

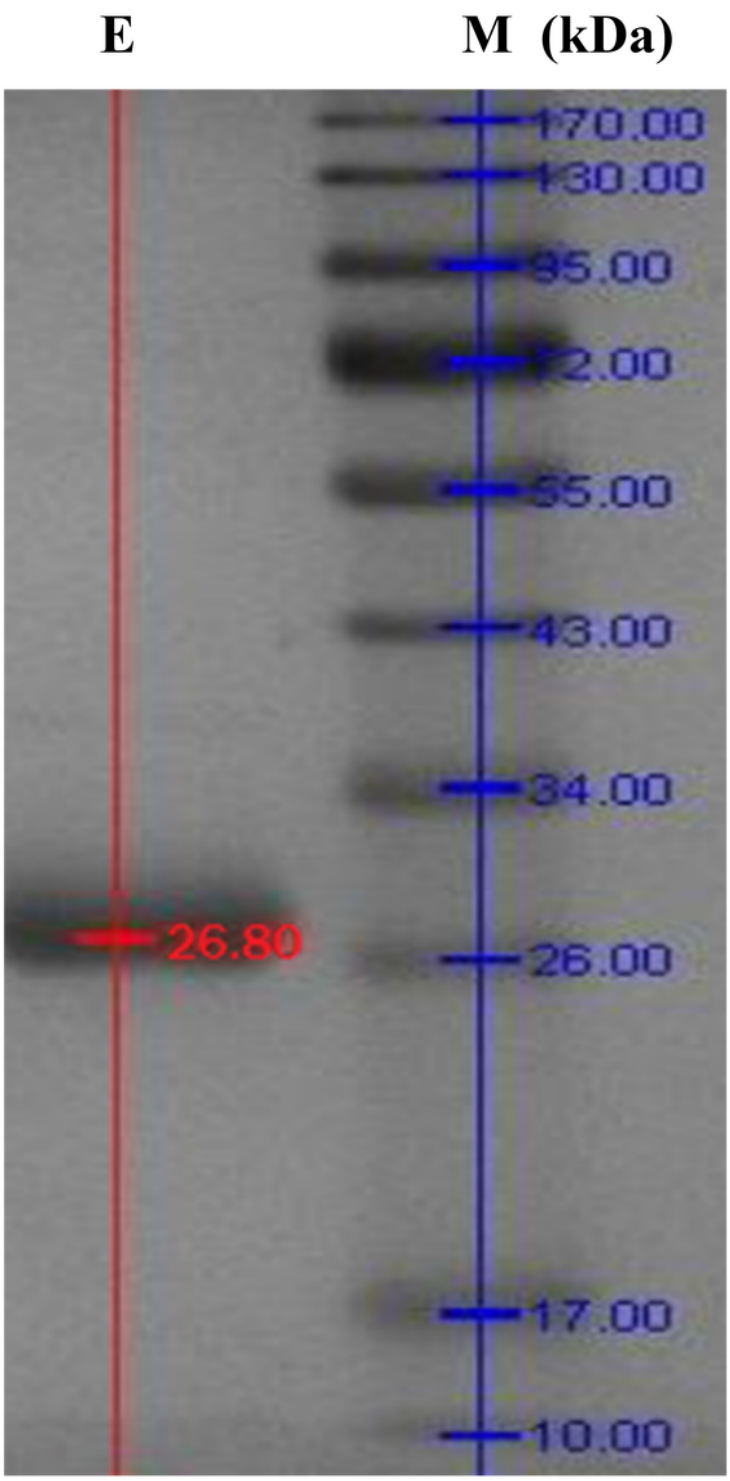

Figure 4

SDS-PAGE display of the purified recombinant thermoalkalophilic esterase from Geobacillus sp. E and M refer to the purified esterase and the protein marker, respectively.

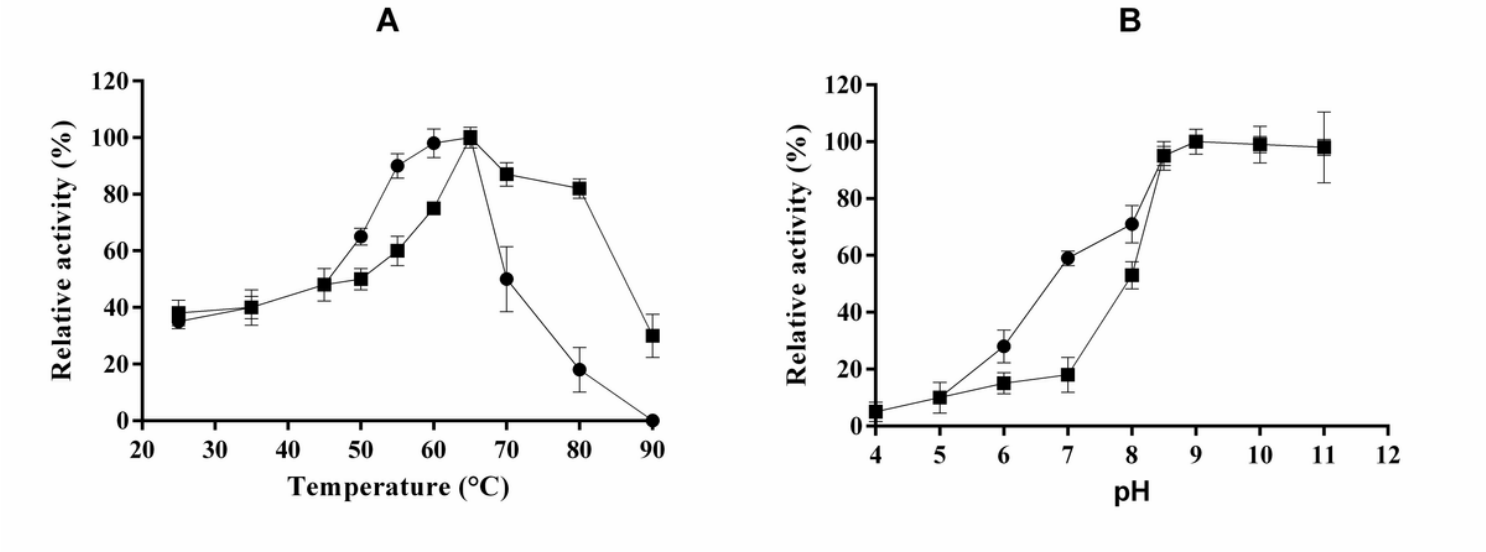

Figure 5

Optimum working temperature (A) and pH (B) of free esterase (●) and the immobilized esterase (■).

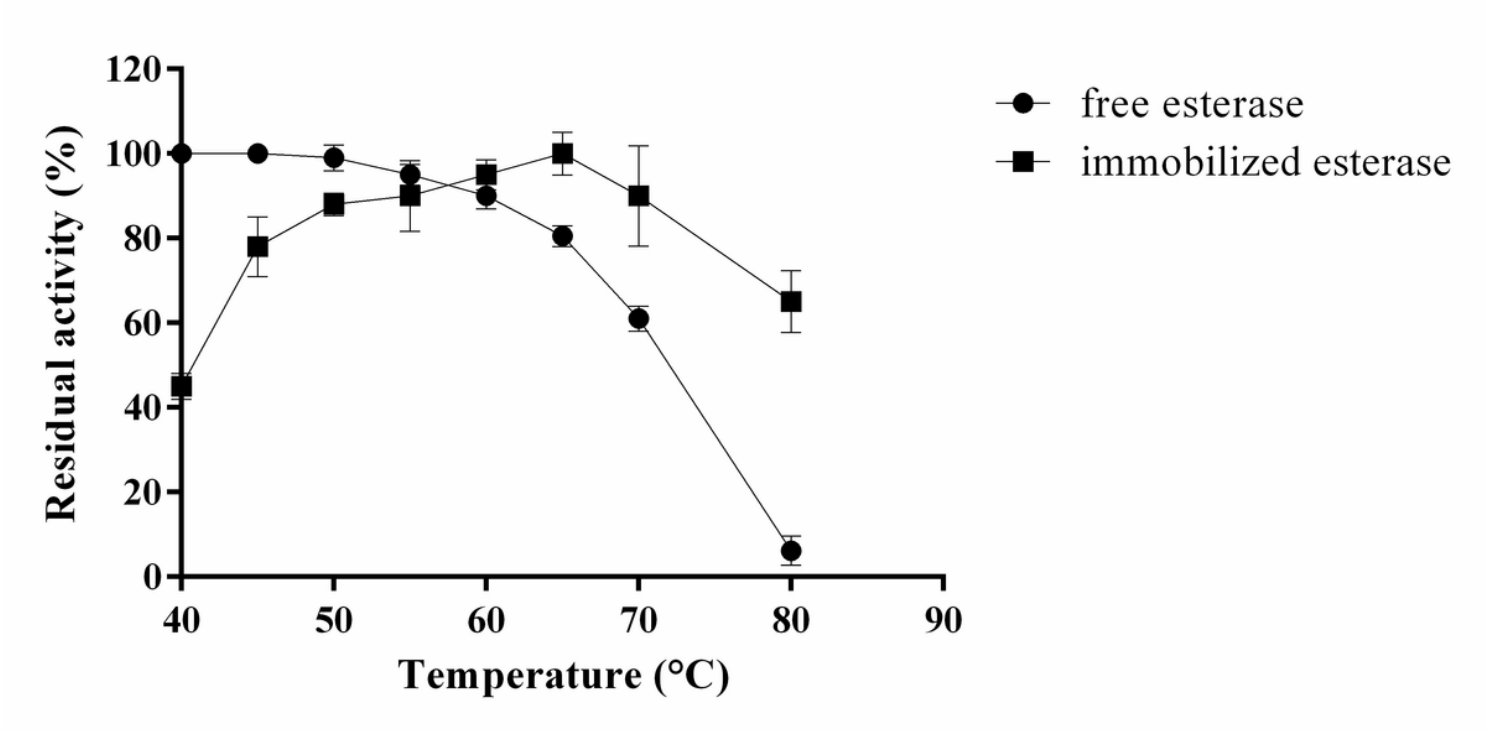

Figure 6

Thermostability of both free and immobilized esterase in the interval of 40-80oC.

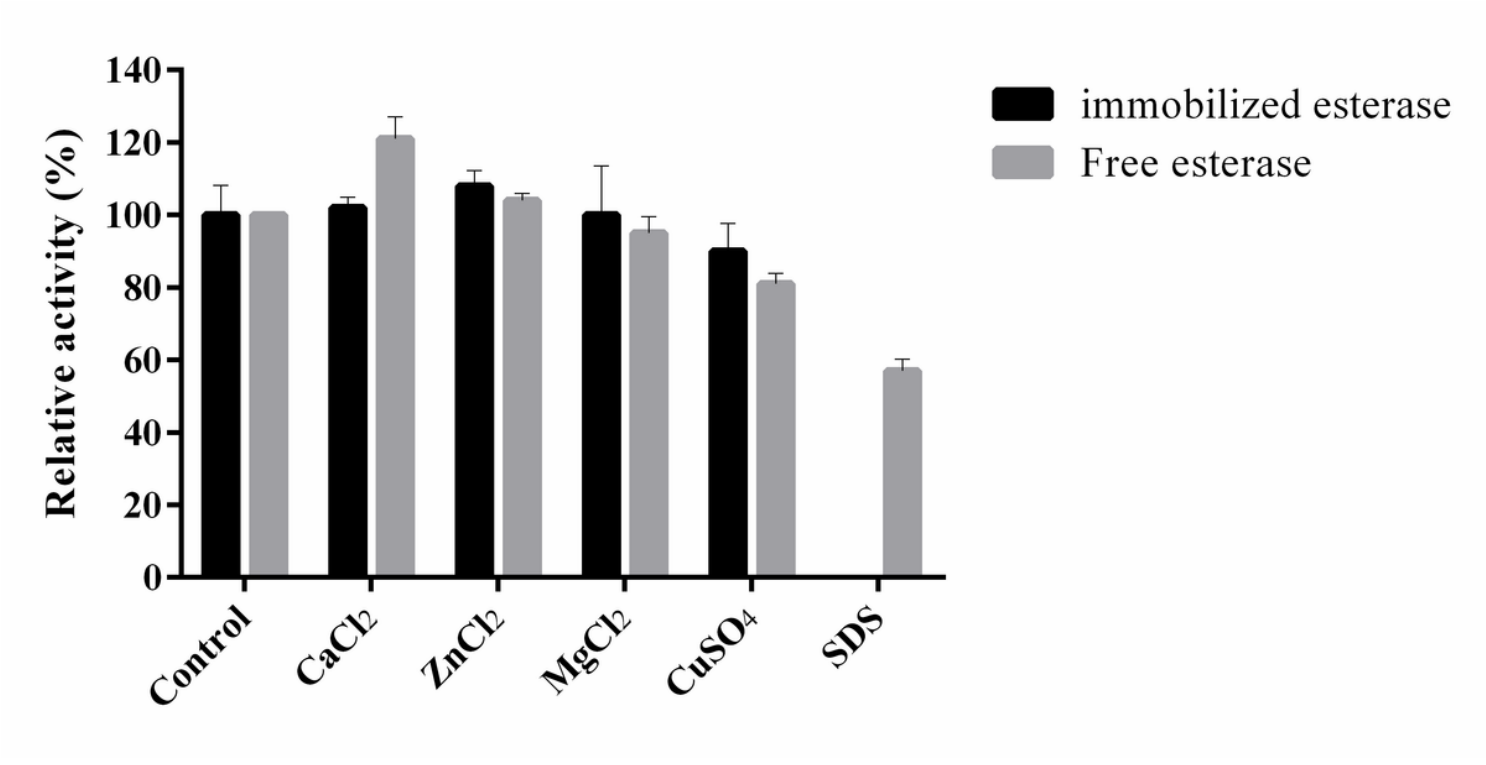

Figure 7

The effect of 1 mM concentration of different metal ions and 1% SDS on the free and immobilized esterase

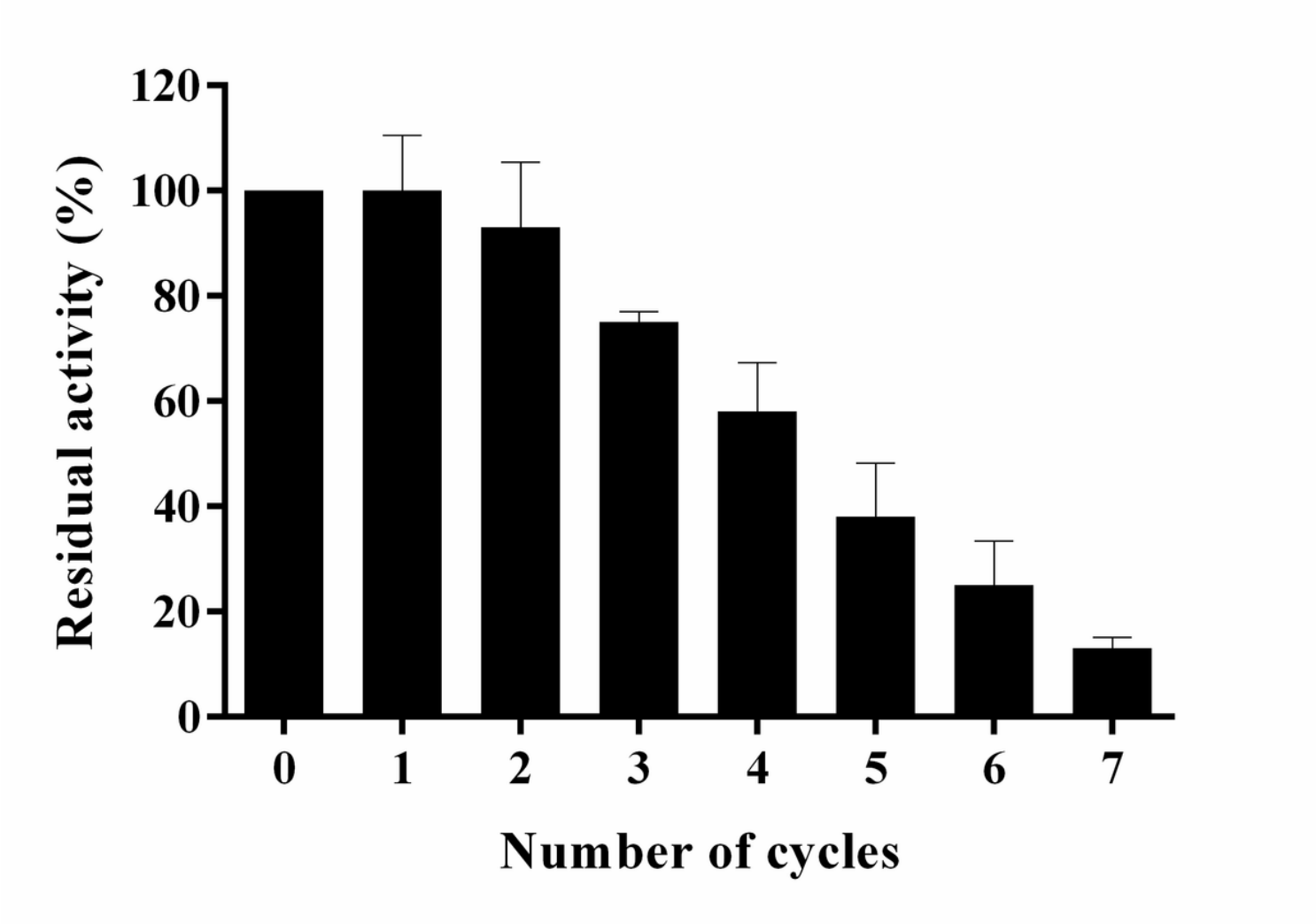

Figure 8

Operational stability of the immobilized esterase during seven sequential cycles.

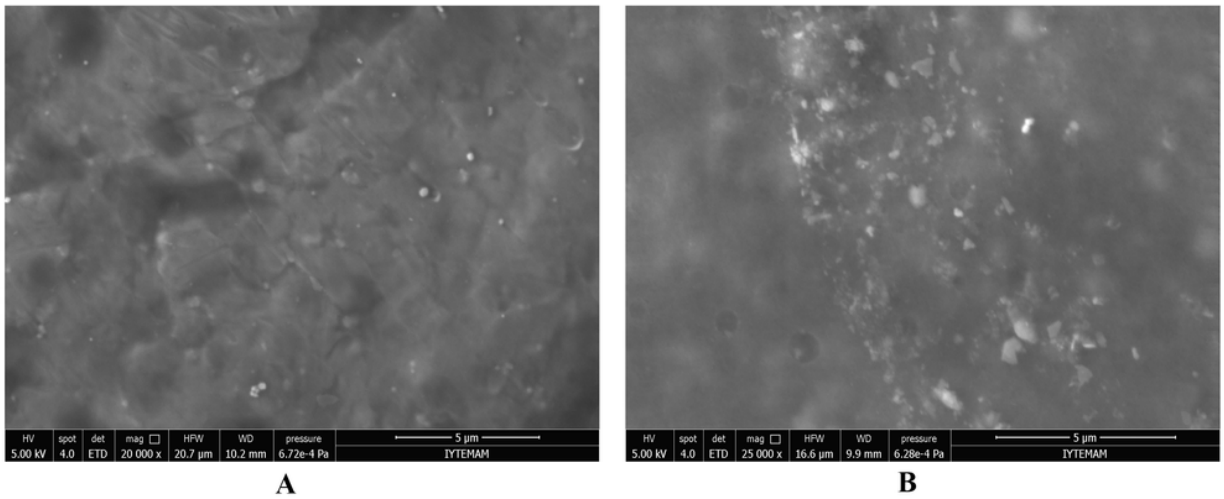

Figure 9

Scanning Electron Microscopy (SEM) images of (A) MCNs and esterase immobilized onto MCNs (B)

Supplementary Files

This is a list of supplementary files associated with this preprint. Click to download.

- GraphicalAbstract8.2.2021ABAB.tif